NONLINEAR DYNAMICS OF A CONTROLLED REVERSE FLOW REACTOR

A. Brasiello[1], L.Russo[2], E.Mancusi[3], M. di Bernardo[4], and S.Crescitelli[1]

[1]Department of Chemical Engineering, University of Naples "Federico II", Piazzale Tecchio 80, 80125 Napoli, Italy.
[2]Department of Chemical and Food Engineering, University of Salerno, via Ponte don Melillo I-84084 Fisciano (SA), Italy.
[3]Department of Engineering, University of Benevento, Piazza Roma, 82100, Benevento, Italy
[4]Dept. of Systems and Computer Science, University of Naples "Federico II", Italy and Bristol Centre of Applied Nonlinear Mathematics, University of Bristol, U.K.

Abstract: A hybrid system approach is adopted to study the dynamic behaviour of a controlled reverse flow reactor in which a feedback control law dictates the occurrence of flow inversions. Typical behaviour of hybrid systems (Zeno phenomena) are found coexisting with other regimes like limit cycles and quasi-periodic regimes. Construction of impact maps, continuation of limit cycles and detection of local bifurcations are employed to understand the influence of Zeno phenomena on bifurcation scenario and on routes to strange attractors.

Keywords: Controlled system, hybrid, Relay control, Non-linear analysis, Regularization.

1. INTRODUCTION

Most exothermic reactions were traditionally conducted in catalytic fixed bed reactors with heat exchangers. Different configurations were introduced to control the evolution of processes; the most commonly used are (1) a simple combination of a separate heat exchanger with an adiabatic reactor; or (2) the integration of either regenerative or recuperative one into catalyst packing of catalytic fixed-bed. Moreover, catalytic processes with low feed concentration cannot be conducted auto-thermally but they need additional heat. An example of this case is the post-combustion of volatile organic compounds (VOC's). In the last few years a new kind of reactors was introduced to sustain exothermic reactions with low feed reactant concentrations: Reverse flow reactors (RFR's) are fixed-bed catalytic reactors in which the flow direction is periodically inverted. In the RFR's, the hot reaction zone is trapped in the packed bed by a periodically reversing of the flow direction (Matros and Bunimovich, 1996). Therefore, it is possible to conduct autothermally the VOC's combustion with lean feed. The main problems relative to the RFR conduction are: overheating of the catalyst and extinction of the reaction. Recently, Barresi and Vanni (2002) propose a simple feedback control (one point controller) which takes into account only the temperature measured by the sensor located close to the inlet at the end of the bed: the flow is reversed when this temperature falls below a fixed value.

In this paper, adopting the control policy of Barresi and Vanni (2002), we analyze the dynamics of closed loop reverse flow reactor for VOC's combustion as set-point variable is varied. The closed loop system is characterized by discrete events (the inversions of the flow direction) and continuous dynamics between two successive switches. So this system is modelled as a so-called hybrid dynamical system (Mancusi, *et al.*, 2004; Schumacher and Van der Schaft, 2000). This kind of systems have been shown to exhibit a rich dynamical behaviour and several peculiar bifurcations that cannot be studied with standard bifurcation theory (di Bernardo, *et al*., 2002).

In this paper, the analysis is carried out using a combination of continuation and numerical simulation of both periodic and complex regimes.

The maximal Lyapunov exponent and impact maps are used to characterize the chaotic nature of a new strange attractor.

2. MATHEMATICAL MODEL

A simple scheme of the catalytic RFR is reported in Fig 1. Two couples of valves (V and W in Fig. 1) allow the reversal of feed flow.

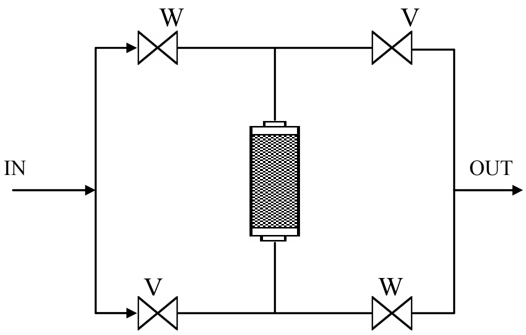

Fig. 1. Scheme of the reverse flow reactor.

Assuming instantaneous inversions, the mathematical model of a one dimensional catalytic RFR with an uniform distribution of catalyst can be written in terms of mass and energy balances, represented by the following dimensionless partial differential equations:

$$\frac{\partial y_g}{\partial \tau} = \frac{1}{Pe_m^g}\frac{\partial^2 y_g}{\partial z^2} + (1-2IO)\frac{\partial y_g}{\partial z} + J_m^g\left(y_s - y_g\right) \tag{1}$$

$$\frac{\partial \theta_g}{\partial \tau} = \frac{1}{Pe_h^g}\frac{\partial^2 \theta_g}{\partial z^2} + (1-2IO)\frac{\partial \theta_g}{\partial z} + J_h^g\left(\theta_s - \theta_g\right) - \varphi\left(\theta_g - \theta_w\right) \tag{2}$$

$$\frac{\partial \theta_s}{\partial \tau} = \frac{1}{Pe_h^s}\frac{\partial^2 \theta_s}{\partial z^2} - J_h^s\left(\theta_s - \theta_g\right) + B\eta Da\left(1-y_s\right)\exp\frac{\theta_s}{1+\theta_s/\gamma} \tag{3}$$

$$J_m^s\left(y_s - y_g\right) = \eta Da\left(1-y_s\right)\exp\frac{\theta_s}{1+\theta_s/\gamma} \tag{4}$$

The mass and heat balances in gas phase (Eqs. (1)-(2)) take in account the mass and heat transport for axial dispersion and convection. The heat balance in solid phase (Eq. (3)) take in account the axial dispersion and reaction. For the mass balance in solid phase (Eq. (4)) a pseudo-steady state is considered.
Mass and heat exchange between two phases and heat exchange between the gas phase and the environment is considered.
Dimensionless parameters and state variables reported in nomenclature are the same adopted by Řeháček *et al.* (1998). Danckwerts boundary conditions are assumed for concentration and temperature in the gas phase:

$$\left.\frac{\partial y_g}{\partial z}\right|_0 - IOPe_m^g y_g\left(0,t\right) = 0 \tag{5}$$

$$\left.\frac{\partial \theta_g}{\partial z}\right|_0 - IOPe_h^g\left(\theta_g\left(0,t\right) - \theta_{feed}\right) = 0 \tag{6}$$

$$\left.\frac{\partial \theta_s}{\partial z}\right|_0 = 0 \tag{7}$$

$$\left.\frac{\partial y_g}{\partial z}\right|_1 - \left(1-IO\right)Pe_m^g y_g\left(1,t\right) = 0 \tag{8}$$

$$\left.\frac{\partial \theta_g}{\partial z}\right|_1 - \left(1-IO\right)Pe_h^g\left(\theta_g\left(1,t\right) - \theta_{feed}\right) = 0 \tag{9}$$

$$\left.\frac{\partial \theta_s}{\partial z}\right|_1 = 0 \tag{10}$$

The variable IO is a discrete variable that can assume only the value 0 or 1. Changing the sign of convective terms inside the equations and inverting the boundary conditions, this discrete variable takes into account that the flow inversions is slaved by the control law.
The control system reverse the flow direction when gas temperature inside the reactor, at a distance equal to 5 cm from the inlet, decrease up to a set-point temperature ($\theta_{\text{set-point}}$):Thus, temperature measurements at each edge of the catalytic bed are needed. If the set point temperature is chosen high enough the controller is able to sustain the reactor auto-thermally. The control law regulates the occurrence of discrete events (the inversions of the flow direction), while the continuous dynamics between two successive inversions is described by the equations (1)-(4): the mathematical model is then a hybrid spatial extended system. Namely, the model is characterized by a discontinuous right-hand side and hence can be classified as a Filippov system (Filippov, 1988).

2.1 The closed loop system as a hybrid automaton.

Because the mathematical model contains both continuous and discrete variable, it can be classified as a hybrid system and can be treated through a formalism called Hybrid automaton which is frequently used for describing and analysing the behaviours of hybrid systems (Johansson *et al.,* 1999). Formally a hybrid automaton is a collection:

$$H = \left(Q, X, Init, f, I, E, G, R\right) \tag{11}$$

where

- Q is the finite collection $\{0,1\}$ of discrete variables;
- X is the collection of continuous variables $x \equiv \left(y_g\left(z,t\right), \vartheta_g\left(z,t\right), \vartheta_s\left(z,t\right)\right)$;
- *Init* is the set of initial states;
- $f: Q \times X \to X$ is the vector field for each $IO \in Q$.
- I assigns to each element of Q the invariant set of all possible values that x can assume;
- E is the collection of edges $\{(0,1),(1,0)\}$;

- G (guard) assigns to each edge the guard condition $\theta_g\left(x_0,t\right)<\theta_{\text{set-point}}$;
- R (reset) assigns to each edge and each $x\in X$, the value that x assumes after the flow inversion.

A hybrid automaton can be equivalently represented by a graph (Fig. 2) that can be easily converted in a numerical algorithm.
The continuous dynamics evolves according to the differential equation specified in each node of the graph. When guard conditions are fulfilled, a discrete transition takes place from one node to another if the nodes are connected by an edge. For more details about the definition of hybrid automaton see Johansson *et al.* (1999).

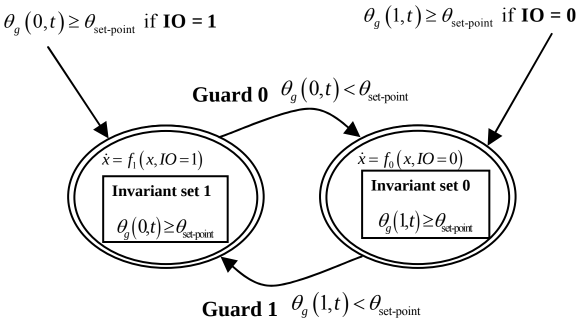

Fig. 2. Hybrid automaton of the controlled reverse flow reactor.

3. RESULTS

The influence of the set point temperature on the dynamic behaviour of the closed loop system is analysed. Varying $\theta_{\text{set-point}}$, the controlled reverse flow reactor shows a very complex behaviour: Zeno phenomena, multiplicity of symmetric and asymmetric regimes, quasi-periodic regimes and strange attractors are observed.

3.1 Zeno executions and multiplicity of regimes.

Hybrid systems allow a particular type of solutions called Zeno executions, which cannot be find in continuous dynamical systems.
Formally, an execution of a hybrid automaton H is a collection $\chi=\left(\tau,x,IO\right)$, where $\tau=\left\{\left[\tau_i,\tau_i'\right]\right\}_{i=1}^{N}$ is a finite or infinite sequence of intervals in which τ_i,τ_i' are the instants of inversions and $\tau_i\leq\tau_i'=\tau_{i+1}$. When $t\in\left[\tau_i,\tau_i'\right[$, IO is constant while x evolves according to the continuous dynamical system (Eqs. (1)-(4)). When $t=\tau_i'$, a discrete evolution takes place governed by the reset map R: $\left(IO\left(\tau_j'\right),x\left(\tau_j'\right)\right)\xrightarrow{R}\left(IO\left(\tau_{j+1}\right),x\left(\tau_{j+1}\right)\right)$.
So the definition of execution involves both the evolution of the continuous variables and the evolution of discrete variables.
An execution is called Zeno if τ is an infinite sequence but $\sum_i\left(\tau_i'-\tau_i\right)<\infty$, in that case $\tau_\infty=\sum_i\left(\tau_i'-\tau_i\right)$ is called Zeno time. Roughly speaking, there is a Zeno execution when a infinite number of discrete transitions (i.e. inversions) occurs in a finite time.
The controlled reverse flow reactor is a hybrid system which admits Zeno executions. A numerical simulation of this phenomenon is reported in Fig. 3.
Physically Zeno state corresponds to a non-ignited regime: To segregate the necessary heat to sustain autothermally the process, control system would switch with infinite frequency.
In all the parameter ranges of interests, the system admits a non-ignited regime. But for $\theta_{\text{set-point}}\geq-7.9$ the extinction of the reaction is reached through a Zeno execution, while for $\theta_{\text{set-point}}<-7.9$ the control does not activate and the reactor admits a non-ignited stationary state, typical of an unforced fixed bed reactor.

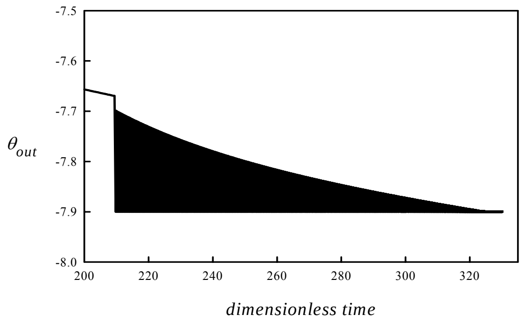

Fig. 3. Temporal series of a Zeno execution of the controlled reverse flow reactor ($\theta_{\text{set-point}}=-7.9$). θ_{out} is the gas dimensionless temperature at *z=1*. In this case Zeno time is $\tau_\infty(X)\approx331$.

Moreover, in the parameter range $\left(-8.10;-7\right)$, these non-ignited regimes coexist with one or more ignited regimes.
Ignited stable periodic symmetric regimes are found in the range $\left(-8.10;-8.07\right)$. The symmetry of these periodic regime is a spatio-temporal one (Russo, *et al.,* 2002) and then it can be expressed by the following relation:

$$x(z,t)=x\left(1-z,t+T/2\right)\qquad(12)$$

where T is the solution period, $T/2$ is the time between two successive switches. Spatial profiles of a symmetric periodic regime are reported in Fig. 4, where it is evident that the profile at instant *t+ T/2* is a mirror reflection of the profile at instant *t*, as dictated by Eq. (12)
In symmetric regimes, two symmetrically placed reactor points (*z* and 1-*z*) experience the same time series but with a time shift equal to $T/2$ (Russo, *et al.,* 2002).
Moreover, for higher parameter values, asymmetric ignited periodic regimes are observed. An example of spatial profiles for asymmetric periodic regime are reported in Fig.5

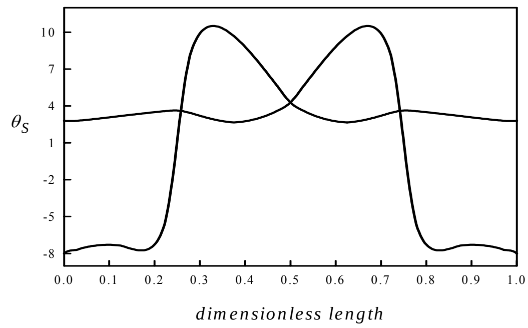

Fig. 4. Spatial solid temperature profiles at time *t* and *t+ T/2* of a symmetric periodic regime.

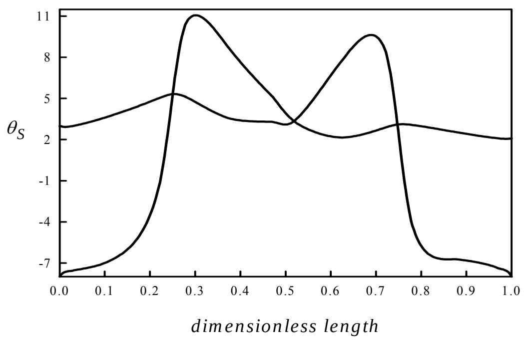

Fig. 5. Spatial solid temperature profiles at time *t* and *t+ T/2* of an asymmetric periodic regime.

It can be observed that asymmetric periodic regimes are characterized by a higher maximum temperature than symmetric regimes. Furthermore, time series at two symmetrically placed reactor points (z and $1-z$), are completely different. So the symmetry-breaking transitions correspond, in some points of the reactor, to sudden increase of temperature and then must to be avoided.

As $\theta_{\text{set-point}}$ is further increased, more complex regimes, like quasi-periodic and even chaotic regimes, occur. To better understand this complex dynamics and to detect the parameter range corresponding to safety operations, a systematic study of limit cycles bifurcations is needed.

3.2 *Continuation of periodic regimes.*

Due to the discontinuity of the vector field, the closed loop system dynamics cannot be studied with standard tools for bifurcation analysis. To overcome this problem the analysis is carried out through the construction of the limit cycles Poincarè map.

Controlled reverse flow reactors can be classified as autonomous systems i.e. neither vector field nor control law depend explicitly on time. Therefore, not only Poincarè maps have a local meaning, but their construction is not trivial because of the difficulties in the identification of Poincarè sections. However, for the analysis of hybrid systems, suitable maps can be defined which are useful to understand the underlying system dynamics (di Bernardo and Vasca, 2000). In our case, the so called impact map can be constructed sampling the state of the system at every switch. Generally, an impact map is not a Poincarè map, but it can be easily show that in this case its second iterate it is.

The stability and bifurcation analysis of limit cycles can been conducted through the study of the fixed points of their Poincarè map. The computation of Floquet multipliers and the bifurcations detection are done coupling the continuation software AUTO (Doedel, *et al.*, 1997) with an external subroutine which computes numerically the Poincarè map as the second iterate of the impact map.

With this numerical technique it was obtained the solutions diagram reported in Fig. 6 where the bifurcation parameter is the set-point temperature. Stable periodic regimes are shown as solid lines, unstable regimes are shown as dashed lines. Only ignited solutions are reported.

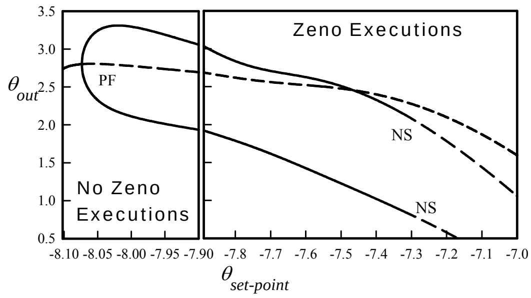

Fig. 6. Solutions diagram of periodic regimes with the set point temperature as the bifurcation parametr. θ_{out} is the gas temperature at z=1.

For low values of the set point temperature, the closed loop reactor exhibits periodic symmetric regimes. As the set point temperature is increased until -8.07, the system exhibits a supercritical pitchfork bifurcation (PF in Fig. 6). As a consequence, the symmetric periodic regime becomes unstable and two stable asymmetric periodic regimes appear. Further increase of bifurcation parameter leads to the appearance, at $\theta_{\text{set-point}} = -7.32$, of a couple of Neimark-Sacker bifurcations (NS) on the two asymmetric periodic branches. In correspondence of these bifurcations, two complex conjugate Floquet multipliers go outside the unit circle: each asymmetric periodic regime becomes unstable leading to an asymmetric quasi-periodic regime. The Poincaré section of a quasi-periodic regime is represented in Fig. 7. Obviously, because of the symmetry of the system, two conjugate quasi-periodic regime coexist.

Asymmetric periodic and quasi-periodic regimes coexist with Zeno executions. This is the first time that this coexistence is observed in a hybrid system. The region of coexistence is reported in Fig. 6. Moreover, as the bifurcation parameter is further increased these quasi-periodic regimes evolves into a couple of strange attractors. When these attractors disappear only Zeno executions are observed by numerical simulations. So, beyond a determined value of set-point temperature ($\theta_{\text{set-point}} \approx -6.9$), the control system is not able to sustain ignited regimes.

3.3 *From quasi-periodic regime to chaos*

In this section the transition is discussed from asymmetric quasi-periodic regimes to strange attractors.
As the set-point temperature is increased, new pieces of invariant sets appear on the Poincarè section, as it is shown in Fig. 8. At the same time, the curve corresponding to the Poincarè section of the quasiperiodic regime, becomes more and more wrinkled (zoom in Fig. 8).

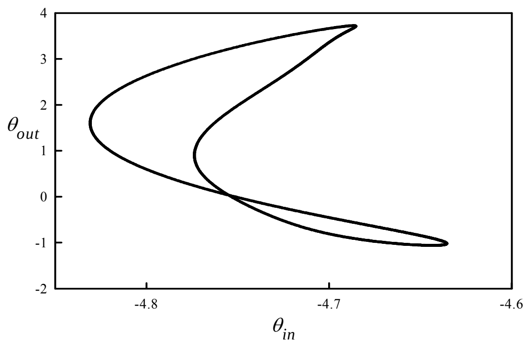

Fig. 7. The Poincarè section of a quasi periodic regime.

These phenomena can be explained as the result of the fractalization of the torus surface where the quasi-periodic solution evolves. Moreover the corresponding maximal Lyapunov exponent is positive (the computations are conducted on the map with the software TISEAN (Hegger, *et al.*, 1999)), and thus these regimes can be classified as chaotic attractors.

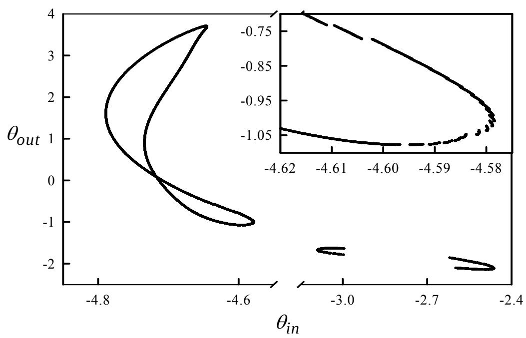

Fig. 8. The Poincarè section of the new chaotic regime.

However, this chaotic regime is not the kind that can be encountered in continuous dynamical systems.
Indeed, in this case, we conjecture that the fractalization is due to the interaction of the quasi periodic regime with the Zeno state. This interaction can be easily recognized looking at the time series reported in Fig. 9. The temporal evolution of the state is characterized by quasi-periodic oscillations (upper figure in Fig. 9) interrupted by high frequencies oscillations like those of a Zeno execution. A zoom of these Zeno-like oscillations is reported in the lower figure in Fig. 9.
Numerical simulations have shown that, as the bifurcation parameter is increased, the frequency of these Zeno-like oscillations grows.

3.4 *Temporal regularization*

Zeno executions are unfeasible in real systems. Typically they are due to modelling abstractions or are related to the control policy (Johansson, *et al.*, 1999). However, they are associated to high frequency switching or chattering, which is undesirable from a practical view point.
In the case of the controlled RFR Zeno phenomena are due to the assumption that the flow inversion is instantaneous. So a way to resolve the Zeno phenomena is to consider a temporal regularization (Johansson, *et al.,* 1999). In many cases, this regularization can be obtained modelling the switching action with a more realistic time delay ε between the time at which the set point valued is reached and the time at which the flow is commanded to switch. A temporal regularization of the closed loop reactor is shown in Fig. 10.

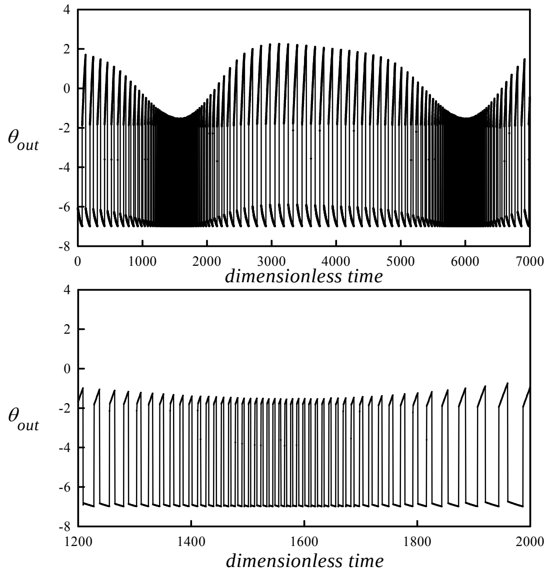

Fig. 9.Time series the new chaotic behaviour (upper figure) and a zoom of the high frequency Zeno like oscillations (lower figure).

As it is apparent in Fig. 10 after a short transient that shows many high frequency switches, the inlet temperature decreases until the extinction of the reaction. The longer the time delay chosen is, the shorter the transient. It is important to stress that, though the Zenoness is removed, a wide time range exists where the closed loop system exhibits many fast switches. Moreover, the dynamics of the controlled reactor is still much complex. Indeed, it is found that temporal regularization doesn’t modify the bifurcation diagram reported in Fig.3. Periodic symmetric and asymmetric periodic regimes as well quasi-periodic and chaotic attractors are still p resent. Furthermore, the temporal regularization does not remove behaviours with Zeno-like oscillations like those reported in Fig. 9.

4. CONCLUSIONS

The nonlinear dynamics of a controlled reverse flow reactor is studied by using a hybrid model of the system and choosing the set-point temperature as a bifurcation parameter. It is known that hybrid systems can exhibit so-called Zeno states. In the case under study, the Zeno state corresponds to a non-ignited regime and its detection has practical relevance. Indeed, the Zeno execution corresponds to operating conditions in which the control law is malfunctioning and unable to achieve the desired control objective. In this paper we show that, in the system of interest,

Zeno phenomena are coexisting with other regimes like limit cycles and quasi-periodic regimes in a wide parameter range. We characterize these limit cycles and their bifurcations with the application of continuation techniques to the impact map of the system.

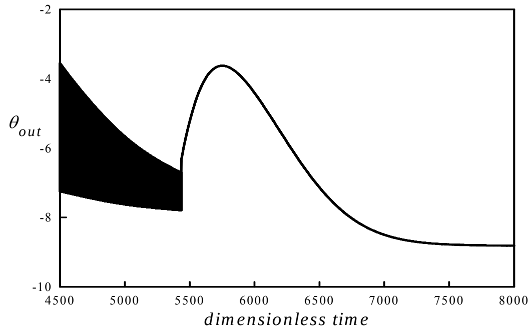

Fig. 10. Temporal series of a quasi-Zeno execution of the regularized hybrid automaton of the controlled reverse flow reactor.

The numerics shown that chaotic behaviour seems to arise as a consequence of the interaction of a quasi-periodic attractor with a coexisting Zeno state. A temporal regularization is adopted to remove the Zeno state, but it is shown not to have an influence on the bifurcation diagram and the nature of the route to chaos observed in the system. Therefore, in order for the control system to induce adequate ignited regimes for the examined process, a suitable start-up policy must be adopted to avoid extinction of reactions or control system breaks. Ongoing work is aimed at a further characterisation of the novel transition reported here involving the coexistence of Zeno points with other stable attractors.

NOMENCLATURE

B adiabatic temperature increase $\Delta H C_{A,in}\gamma / \left(\rho_g c_{pg} T_{in}\right)$

Da Damköler number $L r_{in} / \left(v \varepsilon_s\right)$

θ dimensionless temperature $\tilde{\gamma}\left(\mathrm{T} - \mathrm{T}_{\mathrm{in}}\right) / \mathrm{T}_{\mathrm{in}}$

θ_w dimensionless wall temperature $\left(T_w - T_0\right)\gamma / T_0$

ϕ heat transfer coefficient at the wall $4 h_{fw} L / \left(\rho_{\mathrm{g}} c_{pg} d_r v \varepsilon\right)$

η Effectiveness factor of the catalyst

$\tilde{\gamma}$ Nondimensional activation energy $E / \left(R T_{in}\right)$

J_g^m mass transfer coefficient $k_m a L / \left(v \varepsilon\right)$

J_g^h heat transfer coefficient $h_{fc} a L / \left(\rho_g c_{pg} v \varepsilon\right)$

Pe_g^m Péclet number for mass in gas phase Lv/D

Pe_g^h Péclet number for energy in gas phase $\rho_g c_{pg} L v / k_g$

Pe_g^h Péclet number for energy in solid phase $\rho_s c_{ps} L v / k_s$

y conversion $(C_{in}-C)/C_{in}$

z dimensionless axial coordinate (z*/L)

REFERENCES

Barresi, A. A. and M. Vanni (2002). Control of Catalytic Combustors with Periodical Flow Reversal. *AIChE Journal*, 48, pp. 648-652.

di Bernardo, M., P. Kowalczyk and A. Normack (2002). Bifurcations of dynamical systems with sliding: derivation of normal-form mappings. *Physica D*, 170, pp.175-205.

Doedel, E. J., A. R. Champneys, T. F. Fairgrieve, Y. A. Kuznetsov, B. Sanstede and X. Wang. (1997). AUTO97: continuation and bifurcation software for ordinary differential equations.

Filippov, A. F. (1988). *Differential Equations with discontinuous Righthand Sides*, Kluwer Academic Publisher, Dordrecht.

Hegger, R., H. Kantz, and T. Schreiber (1999). Practical implementation of nonlinear time series methods: The TISEAN package. *CHAOS*, 9, pp. 413-435.

Johansson, K. H., M. Egerstedt, J. Lygeros and S. Sastry (1999). On the regularization of Zeno hybrid automata. *Systems & Control Letters*, 38, pp.141-150.

Mancusi E., Russo L., di Bernardo M. and S.Crescitelli, (2004) Zeno trajectories in a non-smooth model of a controlled reverse flow reactors, European Symposium on Computer-Aided Chemical Engineering: ESCAPE-14, CD-ROM, Lisbon, Portugal, 19-23 May.

Matros, Yu. Sh. and G. A. Bunimovich (1996). Reverse flow operation in fixed bed catalytic reactors. *Catal. Rev Sci. Eng.*, 38, pp.1-68 .

Řeháček, J., M. Kubíček and M. Marek (1998). Periodic, quasi periodic and chaotic spatio temporal patterns in a tubular catalytic reactor with periodic flow reversal. *Comp. Chem. Eng.*, 22, pp.283-297.

Russo, L., E. Mancusi, P.L. Maffettone and S. Crescitelli (2002). Symmetry properties and bifurcation analysis of a class of periodically forced chemical reactors. *Chem. Eng. Sc.*, 57, pp.5065-5082.

Schumacher, H. and A. Van der Schaft (2000). *Introduction to hybrid systems*, Springer-Verlag, New York.

Zhang J., H. Johansson, J. Lygeros and S. Sastry (2001). Zeno Hybrid Systems. *Int. J. Robust Nonlinear Control*, 11, pp 435-451.